

Exclusive Diffractive Electroproduction of Vector Mesons at HERMES

A. Borissov*

on behalf of the HERMES Collaboration

DESY, D-15738 Zeuthen, Germany

E-mail: borissovo@ifh.de

The exclusive diffractive production of light vector mesons (ρ^0, ϕ) at the HERMES experiment with 27.5 GeV beam energy and in the kinematic region $1 \text{ GeV}^2 < Q^2 < 5 \text{ GeV}^2$ and $3.0 \text{ GeV} < W < 6.3 \text{ GeV}$ is described. The longitudinal components of the cross sections are shown in comparison with theoretical calculations based on the Generalized Parton Distributions. In addition, spin density matrix elements (SDMEs) have been determined from exclusive diffractive ρ^0 production. Beam polarization dependent and independent SDMEs have been extracted from the data on hydrogen and deuterium targets accumulated in the years 1996 - 2000. A small but statistically significant violation of s -channel helicity conservation is observed. Kinematic dependence of beam polarization independent SDMEs on t' is presented and compared with available theoretical calculations. An indication is seen of a contribution of unnatural-parity-exchange amplitudes to exclusive ρ^0 production.

DIFRACTION 2006 - International Workshop on Diffraction in High-Energy Physics

September 5-10 2006

Adamantas, Milos island, Greece

*Speaker.

1. Introduction

New and published HERMES data on diffractive vector meson production are presented, and are compared to available theoretical calculations based on the Generalized Parton Distributions (GPDs) [1] which describe dynamical correlations between partons with different momenta. Experimentally, GPDs can be investigated in hard-exclusive production of mesons or non-resonant pion pairs by longitudinally polarized virtual photons. The HERMES longitudinal cross section (σ_L) data on ρ^0 [2] and ϕ meson production have been compared to the GPD based calculations of [3] to estimate the contributions of the two major production mechanisms involved: quark-exchange and gluon-exchange.

The spin transfer from the virtual photon to the vector meson is commonly described [4] in terms of spin density matrix elements (SDMEs). SDMEs are usually described in the center-of-mass system of the virtual photon and target nucleon by the helicity amplitudes $T_{\lambda_V \lambda'_N, \lambda_\gamma \lambda_N}$ where λ_V (λ_γ) is the helicity of the vector meson (virtual photon) and λ_N, λ'_N denote the helicities of incident and outgoing nucleon, respectively. The full expression for the decay angular distribution is given in Ref. [4] in terms of SDMEs r_{ij}^α , which are related to the initial spin density matrix elements $\rho_{\lambda_V \lambda'_V}^\alpha$ of the vector meson: $\rho_{\lambda_V \lambda'_V}^\alpha = \frac{1}{2N_\alpha} \sum_{\lambda_\gamma \lambda'_\gamma} T_{\lambda_V \lambda'_V, \lambda_\gamma \lambda'_\gamma}^\alpha T_{\lambda_V \lambda'_V}^* T_{\lambda_\gamma \lambda'_\gamma}^*$. Here N_α denotes a normalization factor, and $\Sigma_{\lambda_\gamma \lambda'_\gamma}^\alpha$ ($\alpha = 0, 1, \dots, 8$) are nine Hermitian matrices defined in Ref. [4]. The index values $\alpha = 0, 1, 2, 3$ represent transverse photons: unpolarized, the two directions of linear polarization, and circular polarization. Pure longitudinal photons correspond to $\alpha = 4$, and the remaining values $\alpha = 5, 6, 7, 8$ are attributable to the interference of longitudinal and transverse photons. Summation over final nucleon helicities and averaging over initial proton helicities is implied. As the contributions of longitudinal and transverse photons are not distinguishable at fixed beam energy, the alternative matrices (hence-forward referred to as SDMEs) are used [4]: $r^{04} \equiv (\rho^0 + \varepsilon R \rho^4)/(1 + \varepsilon R)$, $r^\alpha \equiv \rho^\alpha/(1 + \varepsilon R)$ for $\alpha = 1, 2, 3$, and $r^\alpha \equiv \sqrt{R} \rho^\alpha/(1 + \varepsilon R)$ for $\alpha = 5, 6, 7, 8$, where ε is the virtual photon polarization parameter and $R \equiv \sigma_L/\sigma_T$ is the longitudinal-to-transverse cross section ratio.

If s -channel helicity conservation (SCHC) is assumed, the helicity of the vector meson is the same as of the virtual photon. The validity of SCHC was tested, and as shown below, the observation of several non-zero SDMEs for ρ^0 production indicates contributions from SCHC-violating helicity-flip amplitudes. In addition, the relative contribution of natural- and unnatural-parity exchange was estimated from the combination of certain SMDEs. Natural-parity exchange indicates that the interaction between the virtual photon and the target nucleon is mediated by a particle of ‘natural’ parity ($J^P = 0^+, 1^-, \dots$ e.g. ρ^0, ω, A_2), while ‘unnatural’ parity exchange denotes the contribution of exchanged mesons with $J^P = 0^-, 1^+, \dots$, e.g. π or A_1 .

2. The cross section of ρ^0 and ϕ production

The ρ^0 and ϕ mesons are observed in the HERMES spectrometer [5] by detecting their decay products in the following channels: $\rho^0 \rightarrow \pi^+ \pi^-$ (100%) and $\phi \rightarrow K^+ K^-$ (49%). The ρ^0 mesons are identified [2] by requiring $0.6 \text{ GeV} < M_{\pi\pi} < 1 \text{ GeV}$, with $M_{\pi\pi}$ being the invariant mass of the $\pi^+ \pi^-$ system. The $\phi \rightarrow K^+ K^-$ background in the ρ^0 spectra is removed by the requirement that $M_{KK} > 1.04 \text{ GeV}$, if the hadrons are assumed to be kaons. The ϕ mesons are selected by requiring

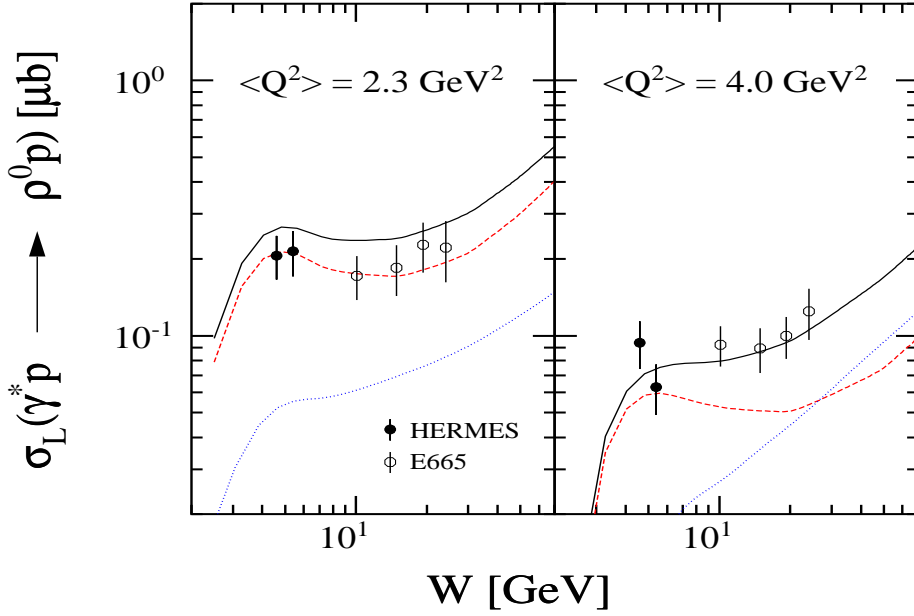


Figure 1: The longitudinal ρ^0 production cross section [2] is compared to the results of calculations based on generalized parton distributions (GPDs). The dotted curves represent the gluon-exchange contribution, the dashed curves the quark-exchange contribution and the solid curves their sum.

$0.99 \text{ GeV} < M_{KK} < 1.04 \text{ GeV}$. The absence of a signal in the Cherenkov detector is required to identify kaon tracks.

For the calculation of the longitudinal cross section [3], higher twist effects have been included in a phenomenological fashion, and the Q^2 -dependence of the strong coupling constant α_s has been accounted for. In order to extract information on the longitudinal production cross section, data on r_{00}^{04} , the longitudinal fraction of the ρ^0 cross section, have been used [2]. Using a parameterization of R the longitudinal cross section for ρ^0 and ϕ production has been determined using $\sigma_L = R\sigma_{total}/(1 + \epsilon R)$, where σ_{total} represents the total measured cross section [2]. The resulting values for ρ^0 and ϕ production are shown in Fig. 1 and the left panel of Fig. 2, respectively, and are compared to the calculations of Ref. [3]. The calculations for ρ^0 are in agreement with the data if both the quark-exchange and the gluon-exchange contributions are included.

For ϕ -meson production only the gluon-exchange mechanism is expected to contribute, as the proton contains only a small population of s -quarks. Calculations based on this assumption [3] are in agreement with the data as presented in the left panel of Fig. 2.

The Q^2 -dependence of the cross section ratio for ϕ to ρ^0 production is displayed in the right panel of Fig. 2, together with the results of other experiments [6, 7, 8]. The ratio of total cross sections shows a clear W -dependence. By contrast, a W -independent ratio of $2/9$ between the total ρ^0 and ϕ production cross sections would be expected if both processes were driven by the gluon-exchange mechanism alone. This is indeed observed for the high Q^2 data which, also correspond to higher values of W . The deviation in the ϕ/ρ^0 total cross section ratio from $2/9$ confirms the conclusions derived from Fig. 1, i.e. that the quark-exchange mechanism represents an important contribution to the ρ^0 production cross section at intermediate W values.

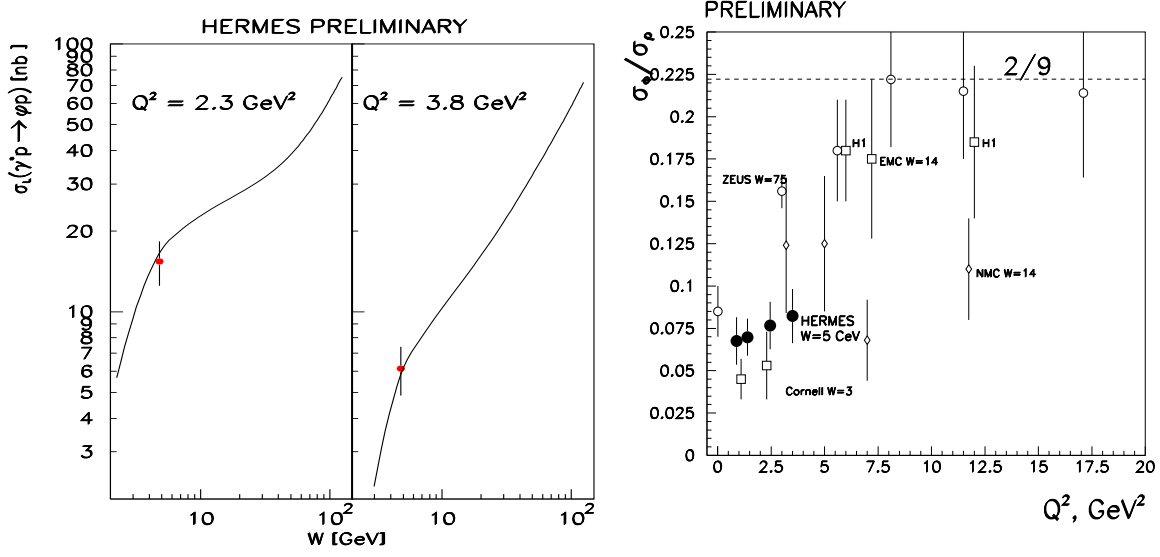


Figure 2: In the left panel the derived longitudinal ϕ production cross section is compared to the results of GPD-based calculations where only the gluon-exchange contribution has been used. In the right panel the ratio of ϕ meson production relative to ρ^0 meson production as a function of Q^2 is presented.

3. Spin Density Matrix Elements

The angular distribution of the scattered lepton and of the decay products is described in terms of the following angles: Φ is the angle between the scattering plane and the ρ^0 production plane, while Θ and ϕ are the polar and azimuthal angles of the decay π^+ in the vector meson rest frame, with the z -axis aligned opposite to the outgoing nucleon momentum in the γ^*p center-of-mass system [4]. The SDMEs are obtained directly from the measured quantities by minimizing the difference between the 3-dimensional $(\cos\Theta, \phi, \Phi)$ decay angle matrix of the data and a sample of fully reconstructed Monte Carlo events, using the maximum likelihood method. An $8 \times 8 \times 8$ binning was used for the variables $\cos\Theta, \phi, \Phi$. The Monte Carlo events were generated with uniform angular distributions and were reweighted in an iterative procedure with the angular distribution $W(\cos\Theta, \phi, \Phi, r_{ij}^\alpha)$ [4], where the matrix elements were treated as free parameters. The best fit parameters were determined using a binned maximum log-likelihood method. The minimization itself and the error calculation were performed using the MINUIT package. All these SDMEs were analyzed without the assumption of SCHC.

The extracted SDMEs for the kinematic region $1 \text{ GeV}^2 < Q^2 < 5 \text{ GeV}^2$, $3 \text{ GeV} < W < 6.3 \text{ GeV}$ and $0.03 < x_{Bj} < 0.25$, are presented for the proton and deuteron data samples in Fig. 3. All unpolarized SDMEs measured on the proton agree with those on the deuteron within one standard deviation of the combined uncertainty. The statistical uncertainties are larger for the eight polarized SDMEs (in the bottom of the plot) due to the limited lepton beam polarization (0.53).

The sections of the central vertical line in Fig. 3 indicate those SDMEs which are expected to be zero under SCHC. The gaps in this line correspond to elements which are not restricted by SCHC to be zero, and which are indeed found to be nonzero. Several unpolarized SDMEs, however, show

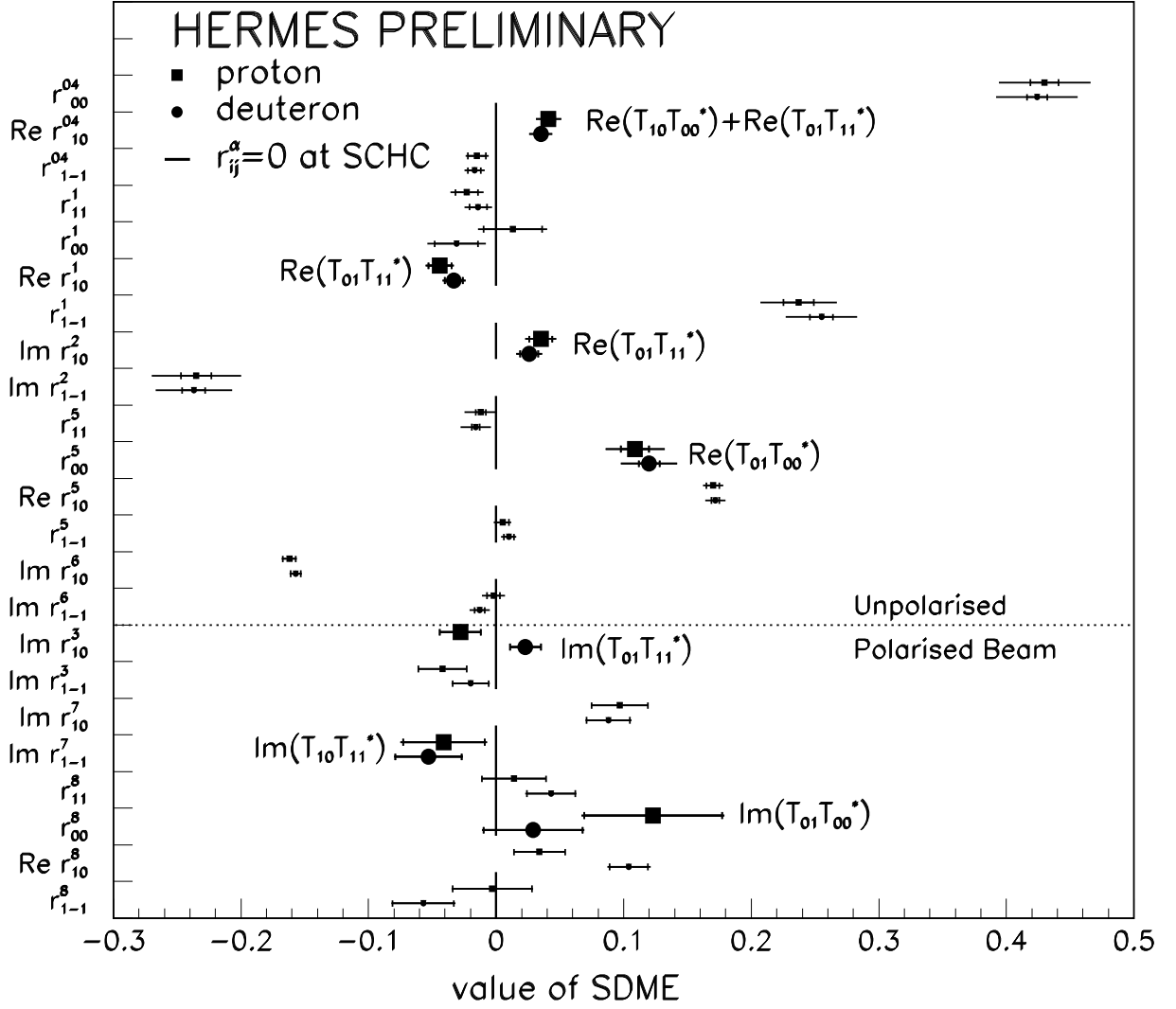


Figure 3: The 23 Spin Density Matrix Elements extracted for ρ^0 production from proton (full squares) and deuteron (full circles) targets. The sections of the vertical line denote the zero predictions for the case of the s-channel helicity conservation assumption. The inner error bars represent the statistical uncertainties as given by MINUIT, while the outer error bars indicate the statistical and systematic uncertainties added in quadrature. Enlarged symbols represent SDMEs violating SCHC; the corresponding spin-flip amplitude is noted beside the points.

significant violations of SCHC. Their offsets from zero are expressed in units of standard deviations as follows (with proton- and deuteron-target results separated by commas): r_{00}^5 : 4.7, 5.5, $\text{Re}\{r_{10}^{04}\}$: 4.1, 3.9, $\text{Re}\{r_{10}^1\}$: 4.0, 3.7, $\text{Im}\{r_{10}^2\}$: 2.9, 2.6. These results indicate a non-negligible contributions of spin-flip amplitudes to exclusive ρ^0 production at intermediate energies.

The t' -dependence of the 15 unpolarized SDMEs obtained for proton and deuteron data in four bins of t' (0 - 0.05 - 0.1 - 0.2 - 0.4) GeV^2 is shown in Fig. 4. It is compared to calculations performed using three different approaches, based on pQCD k_T factorization [10], Regge phenomenology [11], and on a pQCD GPD-based calculations [12]. Only two-gluon exchange is considered in all approaches, and it could be a reason for the disagreement between the data and

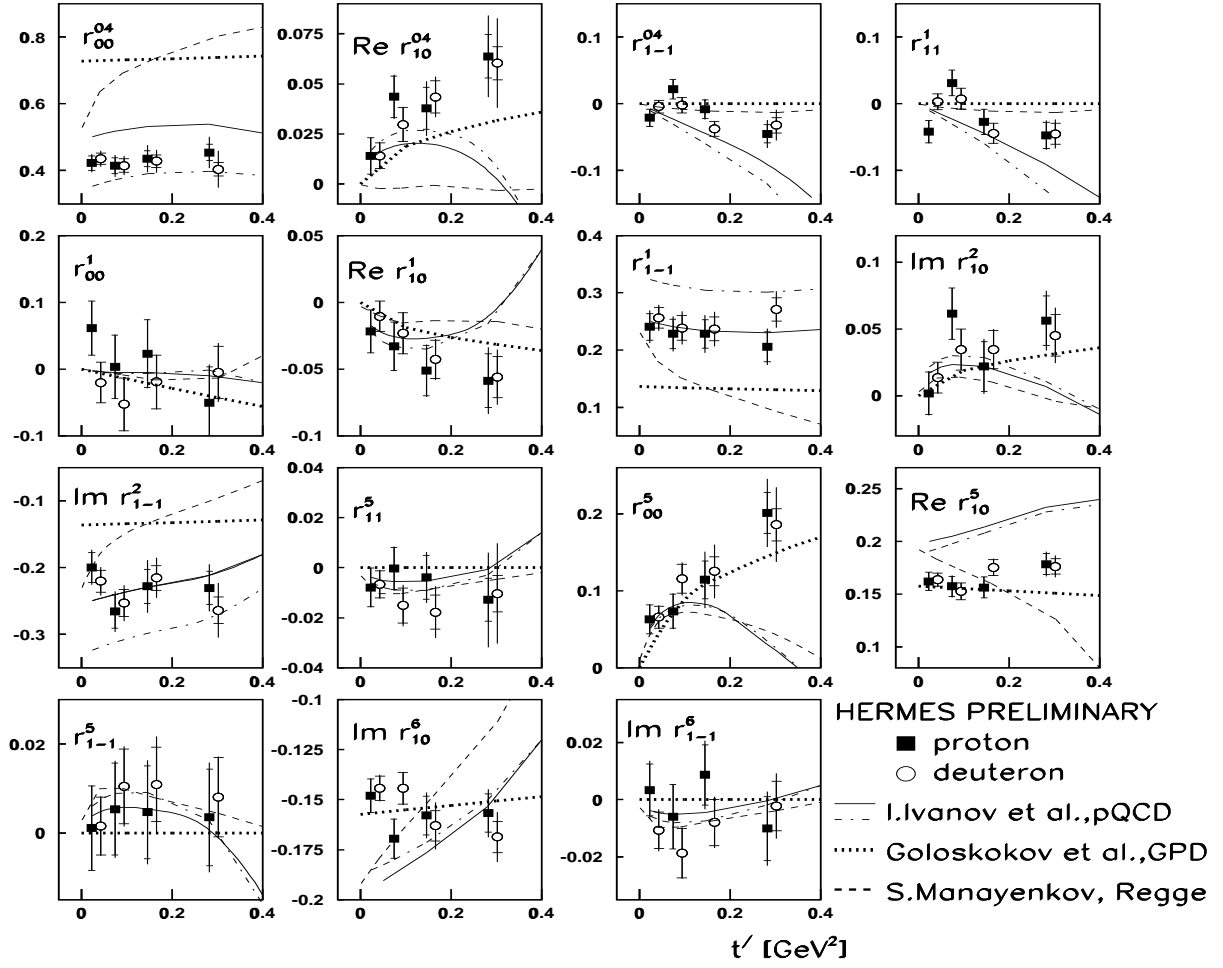


Figure 4: The t' -dependence of the unpolarized SDMEs for proton (full squares) and deuteron (full circles) targets compared with theoretical calculations. The inner error bars represent the statistical uncertainty, while the outer ones indicate the statistical and systematic uncertainties added in quadrature.

the calculations. GPD-based and Regge-phenomenology calculations are planned to include the quark-exchange process in addition to gluon-exchange.

Disregarding the assumption of SCHC, the hypothesis of the absence of unnatural-parity exchange (UnPE) in the t -channel implies that $U_1 \equiv 1 - r_{00}^{04} + 2r_{1-1}^{04} - 2r_{11}^1 - 2r_{1-1}^1 = 0$. The HERMES proton result, $U_1 = 0.112 \pm 0.033_{stat} \pm 0.049_{syst}$, is different from zero at a level of 2σ of the total uncertainty, demonstrating the significance of the unnatural-parity-exchange contribution. The deuteron result is compatible with zero: $U_1 = 0.059 \pm 0.026_{stat} \pm 0.047_{syst}$. For coherent ρ^0 production on the deuteron only NPE is expected, as the isovector contribution is absent in the t -channel, as long as one-pion exchange is considered. A signal of UnPE is important as evidence of quark-antiquark exchange, corresponding to the polarized GPDs. The kinematic dependences of U_1 for the proton on Q^2 , t' and x_{bj} are presented in Fig. 5. Though the errors are large due to the large number of SDMEs involved, all measured values of U_1 are positive.

This work is supported in part by the Heisenberg-Landau program.

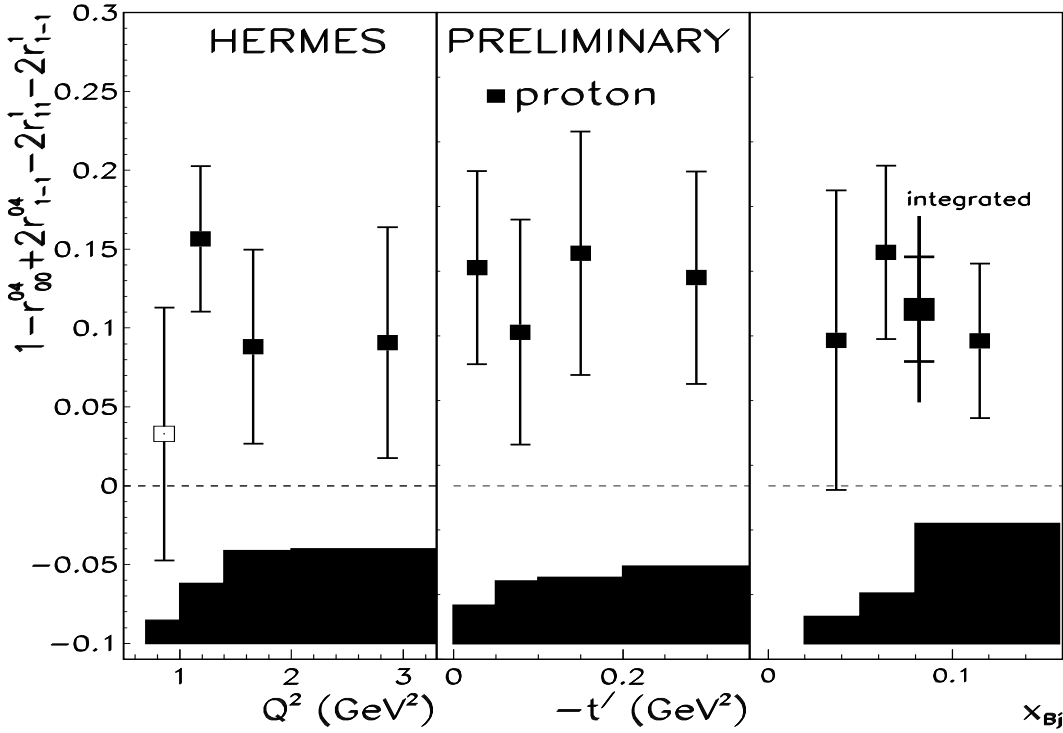


Figure 5: The Q^2 , t' , and x_{Bj} dependence of the combination of SDME's U_1 for hydrogen, which should be zero if only natural parity exchange contributes. The data given in the open point for the first Q^2 bin ($< 1 \text{ GeV}^2$) are not included in the t' and x_{Bj} plots, which represent data with a $Q^2 > 1 \text{ GeV}^2$ imposed. The error bars represent the statistical uncertainty while the bands below indicate the systematic uncertainties. For the integrated point, the inner error bar represents the statistical uncertainty while the outer one indicates the additional systematic uncertainty.

References

- [1] A.V. Radyushkin, Phys. Rev. D **56** (1997) 5524; X. Ji, J. Phys. G **24** (1998) 1181.
- [2] HERMES Collab. K. Ackerstaff *et al.*, Eur. Phys. J. C **17** (2000) 3898.
- [3] M. Vanderhaeghen, P.A.M. Guichon, M. Guidal, Phys. Rev. Lett. **80** (1998) 5064; M. Vanderhaeghen, P.A.M. Guichon, M. Guidal, Phys. Rev. D **60** (1998) 094017.
- [4] K. Schilling and G. Wolf, Nucl. Phys. B **61** (1973) 381.
- [5] HERMES Collab. K. Ackerstaff *et al.*, NIM A **417** (1998) 230.
- [6] D.G. Cassel *et al.*, Phys. Rev. D **24** (1981) 2787.
- [7] M. Arneodo *et al.*, NMC Collab., Nucl. Phys. B **429** (1994) 503.
- [8] M. Derrick *et al.*, ZEUS Collab., Preprints DESY 96-002, 96-067 (1996).
- [9] K.Ackerstaff *et al.*, Eur. Phys. J C **18** (2000) 303.
- [10] I.P. Ivanov, N.N. Nikolaev, A.A. Savin, hep-ph/0501034; DESY preprint 04-243, Submitted to Phys. Element. Part. Atom. Nucl.
- [11] S.I. Manayenkov, Eur. Phys. J C **33** (2004) 397.
- [12] S.V. Goloskokov and P. Kroll, Eur. Phys. J. C **42** (2005) 4492.